Inorg. Chem. **XXXX**, *xx*, 0

Multiple-Timescale Photoreactivity of a Model Compound Related to the Active Site of [FeFe]-Hydrogenase

Anna R. Ridley,[†] A. Ian Stewart,[‡] Katrin Adamczyk,[§] Hirendra N. Ghosh,[§] Boutheïna Kerkeni,[||] Z. Xiao Guo,[||] Erik T. J. Nibbering,[§] Christopher J. Pickett,*[,†] and Neil T. Hunt*[,‡]

Department of Physics, University of Strathclyde, SUPA, 107 Rottenrow East, Glasgow G4 0NG, U.K., School of Chemical Sciences and Pharmacy, University of East Anglia, Norwich NR4 7TJ, U.K., Max Born Institut fuer Nichtlineare Optik and Kurzzeitspektroskopie, Max Born Strasse 2A, D-12489 Berlin, Germany, and Department of Chemistry, University College London, 20 Gordon Street, London WC1H OAJ, U.K.

Received March 31, 2008

Ultraviolet (UV) photolysis of (μ-S(CH$_2$)$_3$S)Fe$_2$(CO)$_6$ (**1**), a model compound of the Fe-hydrogenase enzyme system, has been carried out. When ultrafast UV-pump infrared (IR)-probe spectroscopy, steady-state Fourier transform IR spectroscopic methods, and density functional theory simulations are employed, it has been determined that irradiation of **1** in an alkane solution at 350 nm leads to the formation of two isomers of the 16-electron complex (μ-S(CH$_2$)$_3$S)Fe$_2$(CO)$_5$ within 50 ps with evidence of a weakly associated solvent adduct complex. **1** is subsequently recovered on timescales covering several minutes. These studies constitute the first attempt to study the photochemistry and reactivity of these enzyme active site models in solution following carbonyl ligand photolysis.

The Fe-only hydrogenases reversibly catalyze the reduction of protons to molecular hydrogen. Understanding the chemical basis of this process is of significance to the design of new technological systems for hydrogen production and utilization, and considerable advances have been made in studies of the biochemistry of these enzymes and of synthetic active site models;[1] these have been extensively reviewed.[2,3]

X-ray crystallographic studies of the active site of an Fe-only hydrogenase show a {4Fe4S} cubane structure linked via a cysteinyl bridge to a diiron subsite, a structure previously unprecedented in nature.[4,5] One important facet of the chemistry of the enzyme is the inhibition of catalysis by CO bound to the active site. Studies using irradiation of the CO-inhibited state at cryogenic temperatures have shown evidence for a structure identical with that of the oxidized form of the enzyme, as well as the loss of the infrared (IR) band associated with the bridging carbonyl ligand.[6] Photolysis of diiron carbonyl analogues is thus important in the context of the photolability of CO in the biological hydrogenase system and provides a vital basis for future studies of the enzyme; however, the ultrafast dynamics of these species remains unexplored. Ultraviolet (UV)−Fourier transform IR (FTIR) studies of iron carbonyl sulfide, Fe$_2$(CO)$_6$(μ-S$_2$), in a Nujol matrix show that the two lowest-energy transitions correspond to Fe−Fe bond activation at 450 nm, resulting in a change of the geometry, while higher-energy absorptions (285 nm $< \lambda <$ 420 nm) correspond to metal-to-ligand charge-transfer transitions and result in the loss of a carbonyl ligand.[7] The role of CO loss in the enzyme mechanism makes the latter transition the most pertinent to this study.

To establish the general photochemical behavior of diiron carbonyl dithiolate systems related to the subsite of Fe-only hydrogenase in solution, results of the photolysis of **1** under ambient conditions using ultrafast UV-pump IR-probe techniques and continuous photolysis are presented. UV-pump IR-probe spectroscopy is a well-established technique. Briefly, UV-pump pulses (60 fs duration, $\lambda = 330$ nm) were incident upon the sample, where they were overlapped spatially and temporally with mid-IR pulses (100 fs) with a wavelength resonant with the carbonyl ligand stretching vibrations of **1** (ca. 2000 cm^{-1}). The time delay between pump and probe pulses was variable up to 1 ns using an

* To whom correspondence should be addressed. E-mail: c.pickett@uea.ac.uk (C.J.P.), nhunt@phys.strath.ac.uk (N.T.H.).
† University of East Anglia.
‡ University of Strathclyde.
§ Max Born Institut fuer Nichtlineare Optik and Kurzzeitspektroskopie.
|| University College London.

(1) Evans, D. J.; Pickett, C. J. *Chem. Soc. Rev.* **2003**, *32*, 268.
(2) Liu, X. M. I. S.; Tard, C.; Pickett, C. J. *Coord. Chem. Rev.* **2005**, *249*, 1641.
(3) Capon, J. F.; Gloaguen, F.; Schollhammer, P.; Talarmin, J. *Coord. Chem. Rev.* **2005**, *240*, 1664.
(4) Peters, J. W.; Lanzilotta, W. N.; Lemon, B. J.; Seefeldt, L. C. *Science* **1998**, *282*, 1853.
(5) Nicolet, Y.; Piras, C.; Legrand, P.; Hatchikian, C. E.; Fontecilla-Camps, J. C. *Struct. Fold. Des.* **1999**, *7*, 13.
(6) Chen, Z.; Lemon, B. J.; Huang, S.; Swartz, D. J.; Peters, J. W.; Bagley, K. A. *Biochemistry* **2002**, *41*, 2036.
(7) Silaghi-Dumitrescu, I.; Bitterwolf, T. E.; King, R. B. *J. Am. Chem. Soc.* **2006**, *128*, 5342.

10.1021/ic800568k CCC: $40.75
Published on Web 07/30/2008

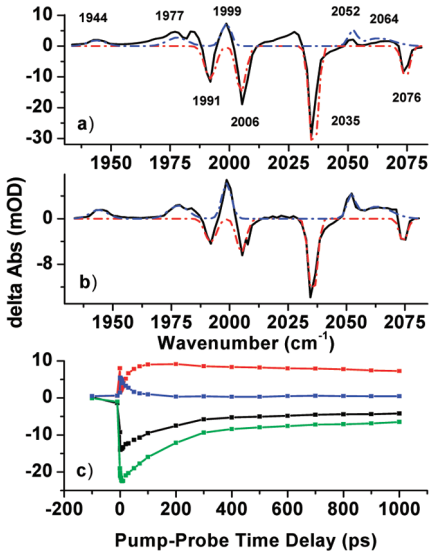

Figure 1. Ultrafast UV-pump IR-probe data. (a) Difference spectrum recorded with a pump−probe delay time of 50 ps. (b) Like part a but with pump−probe delay time = 1 ns. (c) Magic-angle temporal dependence of **1** bleaches at 1991 and 2005 cm^{-1} (black and green), a photoproduct band at 1999 cm^{-1} (red), and cooling effects at 2010 cm^{-1} (blue). In parts a and b, dashed lines are fits to reactant and product spectra (see the text).

optical delay line. Thus, the IR spectrum of the sample was recorded before and after UV irradiation with ultrafast time resolution. Steady-state UV−FTIR measurements were performed by recording FTIR spectra before, during, and after irradiation by a continuous UV light source. A band-pass filter placed in the UV beam restricted the wavelengths used to 350 ± 50 nm to emulate the ultrafast experiments. The samples were heptane solutions of **1**, produced using established methods,[2] with a peak optical density in the CO stretching region of ca. 0.5. Further details on all experimental methods are given in the Supporting Information.

Density functional theory (DFT) structure optimizations and IR vibrational mode calculations were carried out using the *Gaussian03*[8] program employing the Perdew gradient-corrected correlation functional (BP86)[9] and the all-electron valence triple-ζ basis set TZVP of Ahlrichs and co-workers[10] with polarization functions on all atoms. The optimized structures in each case corresponded to singlet states, as expected from the characteristics of the ligands forming the coordination environment of the Fe atoms. Full details are given in the Supporting Information.

The results of the ultrafast photolysis of **1** are shown in Figure 1. Parts a and b of Figure 1 show UV−IR difference spectra recorded at pump−probe time delays of 50 ps and 1 ns. It was observed that, at all positive time delays, negative, bleach signals appeared at 2076, 2035, 2006, and 1991 cm^{-1}, corresponding to the expected IR absorption frequencies of the parent complex[11,12] (the small peak expected at 1982 cm^{-1} was not clearly resolved because of overlap with product bands; see below), indicating the loss of this complex following irradiation. At short pump−probe time delays (<100 ps), a broad-band transient absorption was observed in the range 1940−2075 cm^{-1} attributable to heating effects and vibrational excitation following UV irradiation. No evidence for electronically excited products was observed on any timescales, indicating rapid relaxation to the electronic ground states of parent and photoproduct complexes, whereupon vibrational cooling occurred. The latter manifests itself as a loss of the broad-band transient absorption; the blue trace in Figure 1c shows the temporal dependence of this absorption well away from any observed bleach or photoproduct bands. At pump−probe delay times longer than ∼50 ps, positive peaks due to the appearance of photoproducts were resolved. These appeared at 2064, 2052, 1999, 1977, and 1944 cm^{-1} (Figure 1a,b) and persisted to the experimental time limit of 1 ns. The temporal dependence of these peaks is shown in Figure 1c (red trace). By 1 ns, evolution of the spectrum such as the narrowing and blue-shifting of photoproduct transitions caused by vibrational cooling was complete, allowing separation of parent bleaches and photoproduct bands. These are shown as red and blue dashed lines in Figure 1b and were obtained by fitting Gaussian profiles to the observed lines. These functions were scaled and added to Figure 1a in order to better show the effects of vibrational heating such as the increased amplitude observed near 2025 and 1960 cm^{-1}. No absorptions at frequencies corresponding to bridging CO groups were observed.

When the temporal dynamics are examined in more detail, Figure 1c shows that excitation of the parent complex leads to the immediate appearance of bleach signals (black and green lines in Figure 1c), all of which recover to around 30% of the initial value. This data were recorded with magic-angle pump−probe polarization geometry in order to negate the effects of molecular rotation. Fitting to a biexponential function revealed two timescales, one of ∼150 ps and a longer value of ∼5 ns. The broad-band transient absorption due to hot photoproducts decayed with a single-exponential timescale of 30 ps (blue trace), identical with the rise time observed for each of the photoproduct bands. It is interesting to note the different timescales for recovery of **1** in comparison to photoproduct formation. This suggests that UV excitation leads to rapid relaxation to a photoproduct state following carbonyl photolysis, while molecules not undergoing photolysis relax more slowly to the ground state of the parent complex possibly because of the need to shed excess energy through vibrational cooling. This also accounts for the slower rate of loss of the transient absorption near 2025 cm^{-1} (Figure 1b) in comparison to the broad-band absorption. The former is red-shifted from the parent complex bleach at 2035 cm^{-1} and is attributable to hot parent complex molecules.

Examination of the anisotropy parameter of the bleach signals of the parent complex showed a molecular rotation time of 17 ps, consistent with previous ultrafast 2D-IR studies

(8) Frisch, M. J. *Gaussian 03*, revision C.01; Gaussian Inc.: Wallingford, CT, 2004.
(9) Perdew, J. P. *Phys. Rev. B* **1986**, *33*, 8822.
(10) Schaefer, A.; Huber, C.; Ahlrichs, R. *J. Chem. Phys.* **1994**, *100*, 5829.
(11) Borg, S. J.; Tye, J. W.; Hall, M. B.; Best, S. P. *Inorg. Chem.* **2007**, *46*, 384.
(12) Borg, S. J.; Behrsing, T.; Best, S. P.; Razavet, M.; Liu, X.; Pickett, C. J. *J. Am. Chem. Soc.* **2004**, 126.

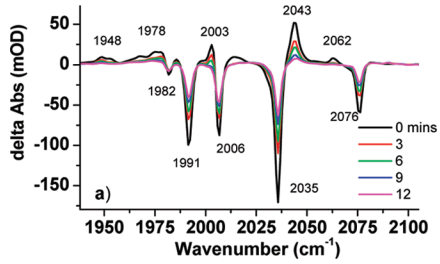

Figure 2. (a) Steady-state UV−FTIR difference spectrum of **1** in heptane at a range of times following 60-s UV irradiation.

of this complex in heptane.[13] Further study of the anisotropy parameters of the CO stretching modes of **1** revealed, by comparison with IR transition dipole moment angular relationships measured by 2D-IR,[13] that the transition dipole moment for the electronic transition lies along the Fe−Fe internuclear bond; this is discussed in more detail in the Supporting Information.

Figure 2 shows the results of 60-s-duration UV irradiation on the FTIR spectrum of **1**. The bleach and photoproduct bands observed are in good agreement with those observed via ultrafast spectroscopy, suggesting that no further chemistry occurs beyond 1 ns. It is interesting to note that turning off the UV source leads to bleach recovery and disappearance of photoproduct peaks, suggesting that the products of the photoreaction are not stable and that the parent complex is recovered. This would be consistent with a CO ligand loss mechanism with no ensuing photochemistry. It can be shown through analysis of the peak integrals that the bleach recovery can be fit using established second-order kinetics,[14] consistent with recombination following photolysis (see the Supporting Information).

To establish the identity of the photoproducts, DFT simulations were used to calculate the structure and IR spectra of three candidate species. These were selected to be (μ-S(CH$_2$)$_3$S)Fe$_2$(CO)$_5$ with an axial or equatorial carbonyl ligand removed and the solvent adduct (μ-S(CH$_2$)$_3$S)Fe$_2$(CO)$_5$(solvent). To increase the computational efficiency, a propane molecule was used for the latter, though it has been shown that the size of the alkane adduct has little effect upon the IR spectrum of the complex.[15]

The results are shown in Figure 3 (for detailed results, see the Supporting Information). It is clear that the IR spectra of the three photoproduct candidates are similar and in good agreement with the observed photoproduct bands. The broad bands observed experimentally near 1950 and 1970 cm^{-1} and multiple bands between 2030 and 2070 cm^{-1} suggest that photolysis leads to a mixture of these three products; this is supported by their similar calculated energies, with the solvent adduct marginally the more stable. Fitting the experimental data to a convolution of the calculated spectra was only moderately successful because of unavoidable

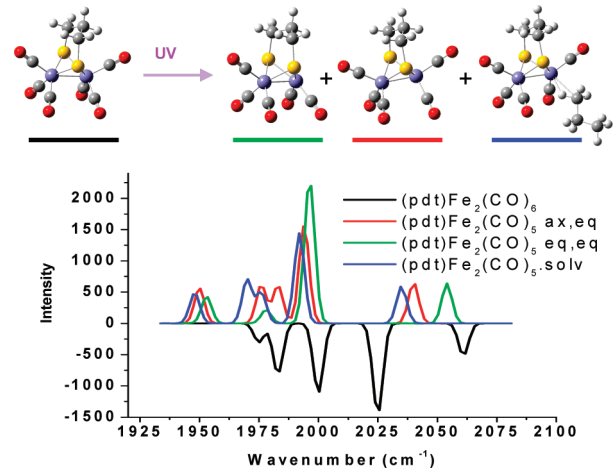

Figure 3. Diagram of the proposed reaction scheme and a summary of the results of DFT calculations on **1** and candidate photoproducts (see the text). Simulation results have been convoluted with a Gaussian line shape to recreate IR spectra. Simulations of the spectra of **1** are shown as bleaches and candidate photoproducts as positive line shapes to facilitate a comparison with experimental data.

errors in calculated intensities and absolute line positions, but the best representations were achieved with approximately equal contributions from all candidate photoproducts (see the Supporting Information), the structures of which are also shown in Figure 3. It is noteworthy that contributions to the FTIR results (Figure 2a) at 2043 cm^{-1} and below 1970 cm^{-1} contrast slightly with the ultrafast data, which show slightly higher frequency contributions. The calculated spectra (Figure 3) suggest that the lower-frequency bands in each region are due to the solvent adduct, and this may imply a shift in the equilibrium toward these on longer timescales in keeping with the greater calculated stability of this species. It is interesting to note, however, that use of a heptanol solvent resulted in similar photoproduct band positions, though resolution was reduced by the broader associated line widths, which suggests weak solvent coordination with the model compound, possibly arising from steric effects.

In summary, irradiation of **1** at 330 nm leads to carbonyl photolysis and the formation of 16-electron photoproducts along with evidence for a weakly associated solvent adduct species (Figure 3), laying the groundwork for future studies of the reactivity of these models of the hydrogenase system.

Acknowledgment. The authors acknowledge EPSRC (Swindon, U.K.) for an Advanced Research Fellowship and a postgraduate studentship (to N.T.H. and A.I.S.) and a postgraduate studentship (to A.R.R.) under the Supergen V Biofuel Cell initiative. EU FP6 Laserlab Europe funding is acknowledged for work carried out at the Max Born Institute (Project mbi001346).

Supporting Information Available: Experimental details and further details relating to analysis procedures as referred to in the main text. This material is available free of charge via the Internet at http://pubs.acs.org.

IC800568K

(13) Stewart, A. I.; Clark, I. P.; Towrie, M.; Ibrahim, S.; Parker, A. W.; Pickett, C. J.; Hunt, N. T. *J. Phys. Chem. B* **2008**, in press.
(14) Steinfeld, J. I.; Francisco, J. S.; Hase, W. L. *Chemical Kinetics and Dynamics*; Prentice Hall: Englewood Cliffs, NJ, 1999.
(15) Cobar, E. A.; Khaliullin, R. Z.; Bergman, R. G.; Head-Gordon, M. *Proc. Natl. Acad. Sci. U.S.A.* **2007**, *104*, 6963.